# *In vitro* studies of DNA condensation by bridging protein in a crowding environment

Sravani K. Ramisetty,[1] Petter Langlete,[1] Rahmi Lale,[2] Rita S. Dias[1]

[1]Biophysics and Medical Technology, Department of Physics, NTNU Norwegian University of Science and Technology, NO-7491 Trondheim, Norway.

[2]Department of Biotechnology, PhotoSynLab, Faculty of Natural Sciences and Technology, NTNU Norwegian University of Science and Technology, NO-7491 Trondheim, Norway.

**Corresponding author:** Rita S Dias, Biophysics and Medical Technology, Dept. of Physics, Norwegian University of Science and Technology, NO-7491 Trondheim, Norway.

Email: rita.dias@ntnu.no, Phone: (+ 47) 73 59 34 22, Fax : (+ 47) 73 59 77 10.

KEYWORDS Histone-like nucleoid structuring protein (H-NS), polyethylene glycol (PEG), synergism.

ABSTRACT The macromolecules of the bacterial cell occupy 20-40 % of the total cytosol volume, and crowded environments have long been known to compact and stabilize DNA. Nevertheless, investigations on DNA-protein binding are generally performed in the absence of crowding, which may yield an incomplete understanding of how nucleoid-assembling proteins work. A family of such proteins, abundant in Gram-negative bacteria, is the histone-like nucleoid structuring proteins (H-NS). Herein, the synergistic role of macromolecular crowding (mimicked using polyethylene glycol, PEG) and H-NS was investigated using fluorescence correlation spectroscopy (FCS) and enzyme protection assays. We show that crowding enhances the binding of H-NS to the AT-rich tracks of the DNA, where it preferentially binds to, protecting these tracks towards enzyme digestion, inducing some DNA condensation, and inhibiting the biological function of DNA. We further suggest that the looping of DNA chains, induced by H-NS, contributes to the synergistic effect of DNA-binding protein and crowding agents, on DNA condensation.

## INTRODUCTION

Genome packaging is a fundamental process accomplished by every living cell during its life cycle, which is vital for conducting all levels of the central dogma in a well-controlled manner. The phenomenon of genome packaging in eukaryotes, consisting of various hierarchical levels of chromatin organization inside the nucleus, is a familiar concept to us that can be found in all biology textbooks. Eukaryotic genomic DNA is packed inside the nucleus by a set of proteins called histones [1] around which the DNA wraps as a first step towards the final X-shaped chromosomal structure. Bacterial cells, on the other hand, lack histone proteins and, thus, well-organized hierarchical levels of genome packaging. Instead, bacteria have its genomic DNA condensed and packed inside the cell as a rosette-like structure called *nucleoid* that occupies 15 %-25 % of the cellular space [2]. Despite extensive efforts by many groups [3-7] to understand the 3D arrangement of bacterial nucleoid, its structure and dynamics are still unclear.

Several phenomena are believed to be involved in DNA condensation within bacterial nucleoid: (i) DNA negative supercoiling; (ii) DNA-binding proteins called nucleoid - associated proteins (NAPs); (iii) less appreciated macromolecular crowding; (iv) DNA charge neutralization induced by cellular polyamines (e.g., putrescine and spermidine) [8-10]; and (v) the recently suggested segregative phase behavior between the genome and other polynucleotides present in the cell [11]. Inside the bacterial cell, DNA is, in a first level, organized in topological domains of about 10 kb in size, resembling a bottlebrush structure [12]. The domain structures are further compacted by the binding of sequence specific or sequence non-specific NAPs. Depending on their structure and binding modes, NAPs can induce DNA bending, bridging, or wrapping. These proteins are thus often called *architectural* proteins [13].

Among the 12 major families of nucleoid-associated proteins present in bacteria; H-NS is one of the most abundant ones. It has attracted much attention due to its role in many processes, such as DNA-binding and genome condensation, gene regulatory function [14], and inhibition of recombination [15]. H-NS binding to DNA is relatively non-specific, when compared to many other architectural proteins, but it seems to show increased affinity towards AT-rich and curved regions of the DNA [16]. H-NS has a molecular weight of 15.6 kDa and pI~7.5 [17, 18], and it is functional in either its dimeric or multimeric form [19]. H-NS binding to DNA has been previously studied using a number of techniques such as atomic force microscopy [20, 21], optical tweezers [22], and computer modelling [23], and is reasonably well established [24, 25].

The large concentration of macromolecules in the cell is believed to have a large impact in many biochemical events including genome condensation. Bacterial cells have 200-300 mg/mL of RNA and protein [26, 27] corresponding to 20-30 % of the total volume of the cell. This reduces the space available to other molecules in the cell, in a phenomenon called 'excluded-volume effect' [28]. Such crowding in a confined cellular environment has a large impact in biochemical, biophysical, and physiological processes such as binding kinetics, polymerization reactions, protein-protein interactions, DNA-protein complexation, and enzyme activity [29-31]. In addition, macromolecular crowding is known to induce the collapse of DNA molecules, the so-called ψ-condensation, as shown both experimentally and theoretically [32-35].

The synergistic role of macromolecular crowding and protein binding on DNA condensation in bacterial cells was first proposed by Murphy and Zimmerman [36]. Here, centrifugation assays followed by gel-electrophoresis were used to show that crowding agents (albumin or polyethylene glycol (PEG) and DNA-binding agents (DNA-bending protein HU or polyamine) jointly reduce the amounts required to achieve DNA condensation. It has been suggested that such synergism is a

consequence of the larger diameter and lower charge density of the protein–DNA filaments as compared to the naked DNA and should be independent of the used proteins [37]. This point was illustrated by showing the synergism of another DNA-bending protein, Sso7d, and PEG on DNA condensation, using centrifugation assays and theoretical arguments [11, 36]. Recently, fluorescence microscopy was used to follow the size of isolated nucleoids in the presence of H-NS and PEG [38]. It was shown that H-NS has little impact on the size of the nucleoids but influenced significantly the nucleoid collapse by PEG.

In this work, we make use of fluorescence correlation spectroscopy to investigate the effect of a reasonably wide range of H-NS and PEG concentrations on DNA conformation. In addition, simple foot printing restriction inhibition assays were performed to gain knowledge on DNA–H-NS interactions in a crowding environment.

## MATERIALS AND METHODS

### Materials

Oligonucleotide primers were received from Sigma-Aldrich. PEG 3000 was purchased from Sigma-Aldrich and used as received. SeaKem$^{R}$ LE Agarose was received from Lonza (Rockland, ME USA), NdeI and NruI restriction endonucleases were from New England bio labs (NEB) and RQ1 RNase free DNase was purchased from Promega (made in USA). The fluorescent nucleotide Alexa Fluor® 488-5-dUTP (490/520 nm) 1 mM stock solution was supplied by Life technologies (Eugene, OR, USA). All stock solutions were prepared in a binding buffer containing 300 mM KCl, 20 mM Tris pH 7.4, 10 mM $MgCl_2$ and prepared using Milli Q deionized water (18.2 Ω/cm resistivity at 25 °C).

### PCR, tagging and purification

A linear double stranded DNA (4145 bp) harboring the gene encoding green fluorescent protein (GFP mut3) under the control of a T7 promoter was generated by polymerase chain reaction (PCR) using the plasmid pSB-E1g (http://dx.doi.org/10.1186/1475-2859-12-26) as the DNA template and forward 5'-GCTGGCCGATAAGCTCTAAG-3', and reverse primers 5'-GGTGCATTGCAAACGCTAGG-3'. After PCR, the product was purified using DNA clean and concentrator kit from Zymogen.

For fluorescence correlation spectroscopy (FCS), the 4145 bp amplicon from the template pSB-E1g was covalently tagged by PCR (using Taq DNA polymerase) with addition of Alexa 488 dUTPs to partially substitute dTTP.

**Protein purification**

H-NS was purified by overexpression in *E.coli* strain ER2566 containing pET21-HNS-cHis6 (generously provided by Prof. William Wiley Navarre of Dept. of Molecular Genetics, University of Toronto, Canada), and grown at 37 °C in Lysogeny broth supplemented with 0.1 mg ampicillin/mL until $OD_{600}$ of 0.6 was reached. H-NS expression was induced by the addition of IPTG (0.1 mM final concentration) and cells were incubated overnight at 18 °C. Protein purification was done as described earlier [39]. In short, the cells were harvested by centrifugation and H-NS was purified using Qian Ni-NTA fast start kit. Purified H-NS protein was buffer exchanged to 20 mM Tris pH 7.2, 300 mM KCl and 10 % glycerol and stored at -20 °C. The H-NS purity was checked by SDS-PAGE and confirmed using MALDI mass spectrometry. Protein concentration was quantified using the Bradford assay with bovine serum albumin as relative standard curve.

**Preparation of DNA–H-NS complexes in the absence and presence of PEG**

DNA–H-NS complexes were prepared by adding equal volumes of DNA and H-NS (totalizing 20 % of the total sample volume), with varying concentrations of H-NS, to the binding buffer (300 mM KCl, 20 mM Tris pH 7.4, 10 mM $MgCl_2$) . Complex formation was allowed for 30 minutes at room temperature. The total volume of sample was typically 50 µL. For samples in crowding conditions, 5 µL of PEG was added to the DNA–H-NS complexes and further incubated for 30 minutes at room temperature. The final concentration of DNA was 2 µg/mL or 5 µg/mL depending on the experimental procedure. A final concentration of 5 % (w/v) of PEG 3000 was used unless mentioned otherwise.

**Electrophoretic mobility shift assay (EMSA)**

DNA–H-NS complexes (5 µg/mL of plasmid DNA in 50 µL and varying concentrations of H-NS) in the absence and presence of PEG, with 4 µL of DNA loading dye were separated on 0.8 % (w/v) agarose gel in the presence of 1×TBE running buffer. Electrophoresis was carried out at 40 V for 5 hrs at 4 °C, and gels were post-stained with Gelred for 1 hr at room temperature and visualized using Bio-Rad Gel Doc™.

**Fluorescence correlation spectroscopy (FCS)**

FCS measurements were conducted using a Leica SP8 confocal fluorescent microscope, with 488 nm Argon excitation laser and a 0.63× water immersion objective. During the experiments we realized that H-NS interacts with fluorescent dyes such as YOYO-I, so, in these studies, Alexa-488 dUTP labelled DNA was used instead. 5 µL of DNA–H-NS complexes in the presence and absence of PEG were placed in silicone isolators on a microscope slide for observation and measurement. This setup allowed working with a small sample volume but also prevented sample evaporation during the measurements. The sample was illuminated with a laser beam and the signal (proportional

to the fluorescence intensity of the sample in the focal volume) was collected by an external single-photon avalanche photodiode (SPAD). Variations in the intensity of the emitted light, corresponding to the movement of fluorescent particles, were used to build FCS autocorrelation curves. Fig. 1 shows an example of such data for labelled DNA. The focal volume was kept constant in all measurements, which implies that the amplitude of the FCS signal is proportional to the amount of fluorescently-tagged DNA in the focal volume. A minimum of 6 autocorrelation measurements, ranging between 50-100 s and averaging 90 s, were recorded for each sample. Autocorrelation functions *G(τ)* were calculated according to the equation

$$G(\tau)=\frac{\overline{I(t)I(t+\tau)}}{\overline{I(t)}^2}-1 \quad ,$$

where *I(t)* is the intensity at time *t* and *τ* is the lag-time. The experimentally obtained curves were fitted with a theoretical correlation $G_t(\tau)$ curve

$$G_t(\tau)=\left[i-T+Te^{-\frac{\tau}{\tau_T}}\right]\sum_{i=1}^{2}(1+\frac{\tau}{\tau_i})^{-1}(1+\frac{\tau}{\tau_i\kappa^2})^{-\frac{1}{2}} \quad ,$$

where *i* is the number of species in solution, *T* is the fraction of molecules in dark state, $\tau_T$ is the triplet lifetime, $\tau_i$, the average diffusion time of the $i^{th}$ diffusing species and $\kappa=\frac{z_0}{w_0}$ is the ratio between the longitudinal and transverse size of the focal volume. Calculation of both autocorrelation functions and the curve fitting was done using the software package SymPhoTime, version 5.3.2.2 from PicoQuant, which also calculates the diffusion constant, according to

$$D_i=\frac{w_0 2}{4\tau_i} \quad ,$$

with $w_0$ the horizontal radius of the focal volume, and the standard deviation $\sigma_{Ti}$ through the bootstrap analysis on the curve fit. A weighted arithmetic mean for the diffusion constant was calculated according to the equation

$$\overline{D}_t = \frac{\sum_{i=1}^{n} \frac{1}{\sigma_{\tau_i}} D_i}{\sum_{i=1}^{n} \frac{1}{\sigma_{\tau_i}}} .$$

Taking the example shown in Fig. 1, and knowing that the average number of diffusers in the focal volume $\langle N \rangle = 0.804 \pm 0.016$, the fitting was best when we assumed two diffusing species with $D_{T_1}$ = 7.68 μm$^2$ s$^{-1}$ ± 0.18 and $D_{T_2}$ = 106.5 μm$^2$ s$^{-1}$ ±13.8. The former is in agreement with previously reported data by Langowski et al. for the diffusion of the DNA molecule of equivalent size [40]. $D_{T_2}$ was found to somewhat vary throughout the studied H-NS concentrations without a significant trend, which led us to assume, together with being a large value, that it corresponds to internal modes of the DNA, free dye molecules, or to the translation mode of primer dimers resulting from the PCR process, although these are not detectable on the gels. $D_{T_2}$ was not taken into account throughout the work. In addition, we have performed a triplet state correction to account for dark states. More details on the fitting procedure and used parameters can be found in the Supplementary Material.

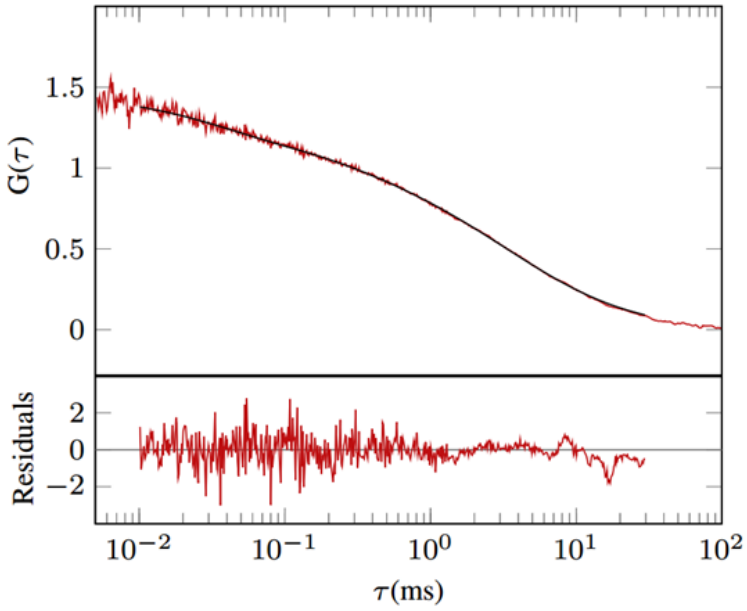


**Figure 1:** Auto correlation function (and corresponding fitting) of a sample containing DNA covalently bound to Alexa-488.

**DNase I (protection) assay**

In order to gain more information on binding of H-NS to DNA, in the absence and presence of PEG, DNase I protection assays were performed. 1 unit of DNase I (defined as the amount required to completely degrade 1 µg of DNA in 10 minutes at 37 °C in the enzyme buffer) was added to the pre-prepared DNA–H-NS or DNA–H-NS–PEG solutions. Samples were incubated for at least 20 minutes at 37 °C to ensure full digestion of the accessible parts of the DNA molecules. All digestions were performed using the binding buffer and not the DNase enzyme buffer. After incubation, samples were evaluated using agarose gel electrophoresis.

**Restriction enzyme digestion assays:**

H-NS has been reported to bind preferentially to intrinsically curved AT-rich regions of DNA. To confirm this and to assess the effect of PEG on the binding of H-NS to DNA, restriction enzymes

NdeI and NruI were added to different DNA−H-NS–PEG reaction mixtures. DNA−H-NS–PEG reaction mixtures were prepared as described above; to these complexes 5 µL of enzyme reaction buffer was added, followed by the addition of the respective enzymes and 1 hour incubation at 37 °C. After incubation, 4 µL of loading dye was added to the reactions and a volume of 10 µL was loaded on 0.8 % agarose gel. Electrophoresis was performed for 1 hour at room temperature. DNA bands were post-stained with Gelred and visualized using Bio-Rad Gel Doc™.

**Atomic force microscopy (AFM)**

Atomic force microscopy was used to visualize DNA–H-NS complexes. Samples were prepared with a final DNA concentration of 2 µg/mL and varied concentration of H-NS in the binding buffer and incubated at room temperature for 30 min.

A 10 µL droplet of DNA–H-NS complex solution was deposited on freshly cleaved high quality mica for <1 min. Then the sample surface was rinsed rapidly with pure water (Milli Q) to obtain a clean surface, and then dried under gentle flow of nitrogen ($N_2$) gas, Imaging was performed in tapping mode™-with a multimode AFM operated by with a Nasoscope controller.

## RESULTS

### Influence of crowding on DNA – H-NS complex formation by EMSA

In order to assess the influence of crowding (addition of PEG) on DNA–H-NS complex formation we started by looking into the binding of H-NS to DNA alone. As seen in Fig. 2, the addition of small concentration of H-NS does not change the mobility of the DNA band (lane 3). As the concentration of H-NS is increased further, we observe a small but visible shift (retardation) of the band (lanes 4 to 8), when compared to that of free DNA (lane 1). This indicates the formation of

DNA–H-NS complexes that have a larger molecular weight and/or the partial neutralization of the DNA phosphate groups due to H-NS binding.

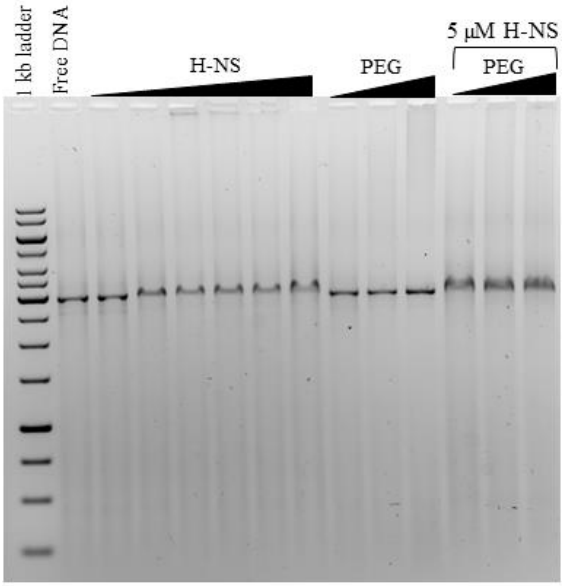


**Figure 2.** EMSA of DNA in the presence of H-NS and PEG for assessment of protein binding to nucleic acid. Lanes 2 to 8 show DNA mobility in the presence of varied concentrations of H-NS (0, 0.5, 1, 5, 10, 25, 50, μM, respectively). Lanes 9 to 11 show the effect of 2, 4, 6 % of PEG on DNA. Lanes 12 to 14 show DNA–H-NS samples, with a concentration of 5 μM of H-NS, and a varied PEG concentration (2, 4 and 6 %). A final concentration of 5 μg/mL of DNA was used.

We have previously seen that synergistic effects are more predominant when the individual condensing species are present in concentrations that lead to none or only partial DNA condensation [41]. Thus, in order to assess the effect of crowding in DNA–H-NS complex formation we have chosen to work further with 5 μM H-NS (lane 5 in Fig. 2). As shown in Fig. 2 lanes 12 to 14, the addition of PEG to the DNA–H-NS complex leads to a small but perceptive change in the band (width and shift) when compared to that of DNA in the presence of 5 μM H-NS (lane 5). The small shift in the DNA–H-NS band suggests that the presence of PEG enhances the binding of H-NS to DNA, and that the complexes do not completely relax to the state prior to PEG addition upon leaving

the well. Control experiments performed with DNA and PEG only (lanes 6-8) do not show a visible shift in the DNA band; PEG is not expected to directly bind to DNA and, being a neutral polymer, it is likely that it will stay in the wells during the electrophoresis run.

**FCS for assessment of crowding effects**

The presence of three different macromolecules (DNA, H-NS and PEG) makes these systems challenging to study. In order to quantify the changes in diffusion of DNA in the presence and absence of crowding molecules, FCS was performed.

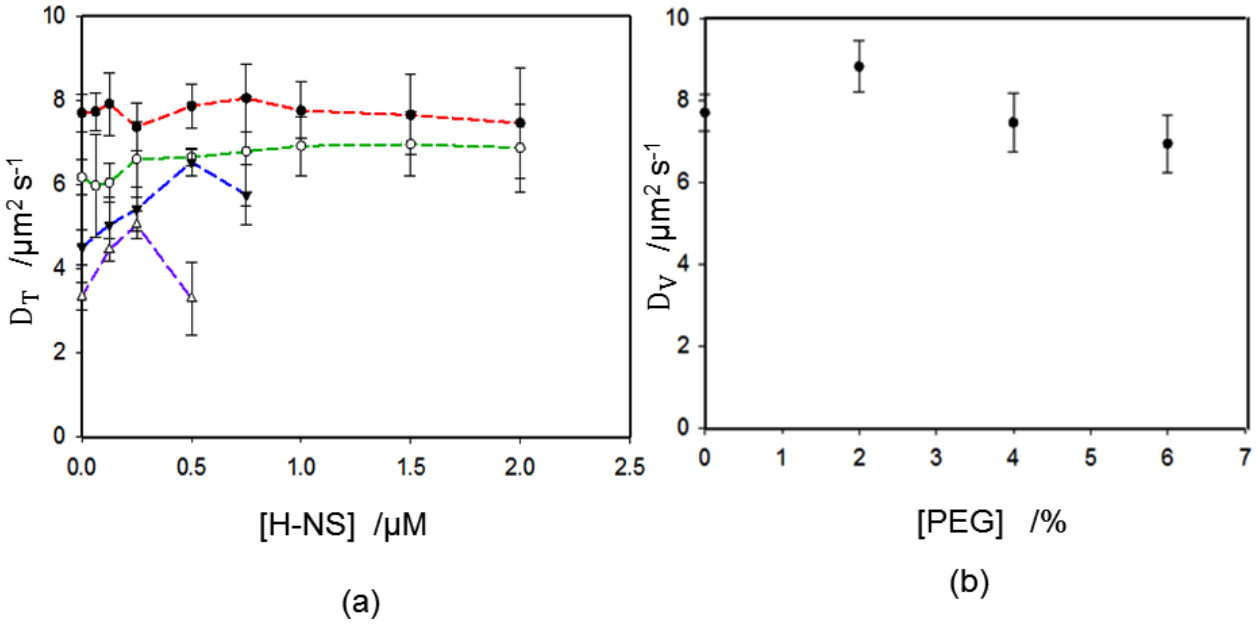


**Figure 3.** (a) Translational diffusion coefficient, $D_T$, of DNA molecules covalently-labelled with Alexa-488 versus the concentration of H-NS, for concentrations of PEG: 0 (filled circles, red line), 2 (open circles, green line), 4 (filled triangle, blue line) and 6 % (open triangles, purple line). Lines are guides to the eyes. (b) Viscosity-corrected diffusion coefficient, $D_V$, of covalently-labelled DNA versus the concentration of PEG. Error bars indicate standard deviation of triplicates. DNA concentration was 2.25 ng/μL.

The translational diffusion coefficient, $D_T$, of the covalently-labelled DNA in the presence of increasing concentrations of H-NS, is shown in Fig. 3a (filled circles and red curve). As can be seen, the measurement of several sets of samples indicates that the presence of H-NS protein induces only a mild to no condensation of DNA.

Fig. 3a additionally shows the effect of crowding molecules on the diffusional behavior of DNA. An initial observation is that $D_T$ decreases with addition of PEG, in the absence of H-NS (first point in each curve of Fig. 3a). Upon increase in the concentration of H-NS we see that, for low concentrations of PEG (2 %, open circle and green curve), there is no significant variation of $D_T$ but, interestingly, when the concentration of PEG is further increased, addition of H-NS leads to a clear increase in $D_T$ of DNA (blue and purple curves), which is consistent with a decrease in the dimensions of the DNA–H-NS complexes. Further addition of H-NS leads to a decrease in $D_T$ due to the aggregation of DNA–H-NS complexes, which were also clearly visible in the microscopic mode (not shown). Similar DNA aggregation behavior under crowded conditions was (in the absence of proteins) described recently using the same technique [42].

The presence of PEG results in a significant increase in the viscosity of the solution, which induced the observed decrease in $D_T$ with increase in PEG concentration. A simple viscosity correction was performed using

$$D_V = D_T \frac{\eta}{\eta_0},$$

where $\eta$ is the viscosity of the PEG solution and $\eta_0$ the viscosity of the buffer. These were estimated by measuring the translational diffusion of rhodamine (R6G) in the binding buffer and various PEG concentrations, and assuming that the size of rhodamine does not change with the concentration of PEG. It is also assumed that the diffusions of R6G and DNA are equally affected by the viscosity of the medium, which according to Ref. [42] is reasonable, taking into account the size and

concentration of the used PEG. Fig. 3b shows the viscosity-corrected translational diffusion, $D_V$, of DNA in the presence of PEG, which now shows no significant variation of the diffusion of DNA with the PEG concentration. This is somewhat surprising, as we would expect that under these conditions PEG would induce condensation of some DNA molecules; dye exclusion assays show that about 30% of the dye is excluded from DNA under these crowding conditions (Fig. S1).

Table 1 shows the values of $D_V$ of DNA in samples with varying concentrations of both H-NS and PEG, now also normalized to the diffusion of DNA alone in the binding buffer, $D_{V,0}$, for easier reading. As discussed, it is seen that increasing amounts of H-NS, in the absence of PEG, have little to no effect on $D_V$ of DNA (first column in Table 1), as do increasing concentrations of PEG alone (first row in Table 1). As for the ternary systems, it is clearly shown that increasing the concentration of H-NS in the presence of PEG leads to an increase in the mobility of the DNA–H-NS complexes (as seen from the increase in $D_V/D_{V,0}$). Factors that affect the diffusion coefficient of a molecule in solution are the hydrodynamic radius, molecular weight and shape of the molecule, the viscosity of the solvent, and the temperature. These experiments were performed at constant temperature throughout the experimental set up. Increasing PEG concentration results in increased viscosity of the system, as discussed, and an effort was made to normalize the samples towards the viscosity. Nevertheless, each sample set has the same viscosity (same PEG concentration) so we can safely look at the trends within these. We are thus left with the properties of the macromolecule that we are following, DNA. Association of H-NS to DNA will lead to an increase in the molecular weight of the DNA–H-NS complex, leading to a decrease in the $D_v$. This effect has been ignored here. The only changes that can contribute to an increase in $D_v$ are a decrease in the hydrodynamic radius and/or the formation of more spherical complexes, both consistent with condensation of the DNA.

The values marked in red in Table 1 indicate the formation of large aggregates. It is worth mentioning that similar systems have shown that DNA condensation is immediately followed by the aggregation of the complexes, due to the (at least) partial neutralization of the DNA molecules (see for example [43]). As discussed above, it is not surprising that aggregation is more pronounced in the presence of a crowding environment.

**Table 1.** Heat map of the viscosity-corrected translational diffusion coefficients of labelled DNA with varying concentrations of H-NS and PEG, normalized to the viscosity-corrected translational diffusion coefficient of DNA alone, $D_V/D_{V,0}$.

| | $D_v/D_{v,0}$ | | | |
|---|---|---|---|---|
| [H-NS] /μM | 0 % PEG | 2% PEG | 4% PEG | 6% PEG |
| 0.000 | 1.00±0.06 | 1.15±0.08 | 0.97±0.09 | 0.90±0.09 |
| 0.063 | 1.00±0.06 | 1.09±0.13 | 1.15±0.09 | 0.91±0.07 |
| 0.125 | 1.03±0.10 | 1.12±0.09 | 1.08±0.14 | 1.20±0.07 |
| 0.250 | 0.96±0.07 | 1.23±0.17 | 1.16±0.11 | 1.36±0.09 |
| 0.500 | 1.02±0.07 | 1.23±0.04 | 1.40±0.07 | 0.89±0.24 |
| 0.750 | 1.05±0.11 | 1.26±0.24 | 1.24±0.16 | - |
| 1.000 | 1.01±0.09 | 1.29±0.13 | - | - |
| 1.500 | 0.99±0.12 | 1.29±0.14 | - | - |
| 2.000 | 0.97±0.17 | 1.28±0.19 | - | - |

Red color indicates samples where aggregation was visible.

## DNA protection towards digestion

The results presented so far show solely a mild condensation of DNA by H-NS binding. We decided thus to evaluate the availability of DNA (in the DNA–H-NS complex) towards digestion by a number of enzymes. DNA–H-NS complexes were treated with DNase I enzyme and the degree of DNA digestion was evaluated using agarose gel electrophoresis (Fig. 4). Since the buffer conditions (e.g., ionic strength, presence of divalent ions) affect the DNA condensation behavior in the presence of DNA-binding and/or crowding agents [41], all samples in Fig. 4 were prepared in the absence of

the DNase enzyme buffer. This did not affect the digestion ability of the DNase I as seen in lane 2, which shows that the DNA band disappears while a broad and faint band, corresponding to small DNA fragment, appears. Addition of increasing concentrations of H-NS leads to some protection, as shown by the increase in the intensity of the band and a shift to larger molecular weights. This indicates that H-NS partially protects DNA, but does not bind to it in a regular fashion.

In order to check the degree of protection of DNA–H-NS complexes in the presence of crowding, a series of reactions with DNA, varying H-NS concentrations, and 5 % of PEG were incubated with DNase I. Lanes 8-12 in Fig. 4 show that the presence of crowding molecules results in near complete protection, even for the lowest studied concentrations of H-NS, which on its own showed no protection. Control experiments with PEG alone were also performed and complete DNA digestion was observed (last lane). The latter observation is in good agreement with the FCS results described above, which show that there is no significant condensation of the DNA at the studied PEG concentration. This is also in good agreement with experiments conducted with larger PEG molecules and the restriction enzyme HindIII, where DNA digestion still progress at 6.25 % but is inhibited with 12.5 % of PEG [42].

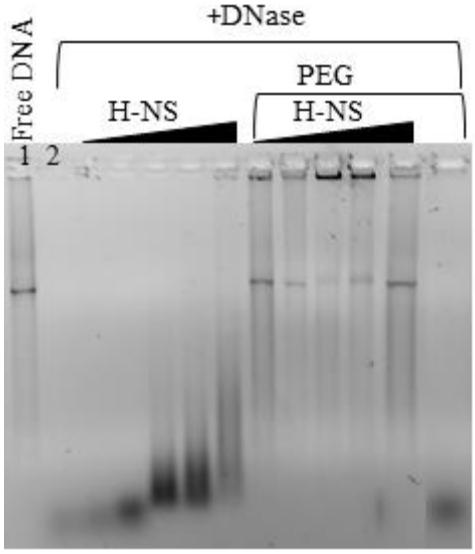


**Figure 4.** DNase I protection assay. To examine binding activity of H-NS to linear plasmid DNA, DNase I digestion reactions were carried out at increasing concentrations of H-NS (0.5, 1, 5, 10, 25 μM) in the absence (lanes 3 to 7) and presence of 5 % PEG (lanes 8 to 12). Lanes 1 and 2 correspond to controls of free DNA with and without enzyme addition, respectively, and the last lane, 13, shows the digestion of DNA in the presence of 5 % PEG (this lane is from the same gel but the order has been changed for clarity). A final concentration of 5 μg/mL of linear plasmid DNA was used for all reactions.

**H-NS prefers A/T and curved regions near the promoter regions:**

Several studies have shown that H-NS binds preferentially at the AT-rich and curved regions of DNA which, not coincidently, are a characteristic of the -10 and -35 region of the promoter [44-46]. Inspired by the mentioned studies, and in order to gain further insight into the effect of crowding on the specificity of H-NS binding to DNA, we have performed a series of simple DNA foot printing assays using two different restriction enzymes, NdeI that selectively cleaves DNA upstream of the promoter region, which is curved and rich in AT-rich sequences, and NruI that selectively cleaves a site downstream of lac operon region at 788 bp that has a large content of GC base pairs (see complete map of the linear plasmid and DNA curvature prediction in Figs. S2 and S3, respectively). DNA–H-NS complexes, in the absence (Fig. 5a) and presence (Fig. 5b) of crowding media (PEG), were incubated with NdeI and loaded on 0.8 % agarose gels. Under optimal conditions NdeI cleaves

DNA into two fragments, one with ~2500 bp and the other with about 1500 bp, as can be seen in lane 3 of Fig. 5a. The same figure shows DNA–H-NS complexes, prepared with different H-NS concentrations in the absence (lanes 4 to 9) and presence (lanes 10 to 15) of PEG. Lane 16 shows a DNA-PEG control sample. These samples were prepared in the presence of enzyme reaction buffer since the digestion was not successful in its absence. Nevertheless the reaction buffer did not interfere significantly with the DNA-H-NS complexes as seen in bands 4 to 9, where the small shift of the DNA is consistent with that shown in Fig. 2. Fig. 5b refers to the same samples as in Fig. 5a, now incubated with the NdeI restriction enzyme. We can see that even at the lowest studied H-NS concentrations (0.5 and 1.0 μM, lanes 2 and 3) most of the DNA is protected towards digestion and only a small amount of DNA is digested, as indicated by the low intensity bands with sizes corresponding to those of the digestion fragments. When the H-NS concentration is increased further, the fragments disappear and we see full protection of the cleavage site for NdeI. When crowding media (PEG) is added to DNA–H-NS complexes (lanes 8 to 13 in Fig. 5b), we observe instead a complete protection of the DNA even for the two lowest H-NS concentrations.

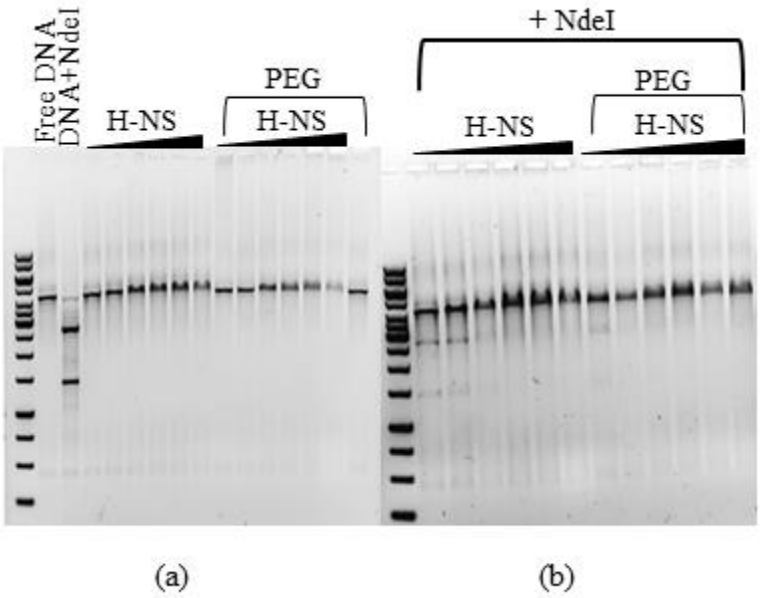


382

383 **Figure 5.** DNA foot printing assay. (a) Agarose gel electrophoresis of linear DNA with increasing H-NS
384 concentration 0.5, 1.0, 2.5, 5.0, 7.0, 10.0 µM in the absence (lanes 4 to 9) and presence (lanes 10 to 15) of 5
385 % PEG. Lanes 1, 2, 3, and 16 (last) correspond to the ladder, free DNA, DNA treated with NdeI, and DNA-
386 PEG, respectively. (b) Agarose gel showing equivalent samples of DNA–H-NS and DNA–H-NS–PEG
387 systems now treated with NdeI enzyme. Lane 1 shows the ladder. A final concentration of 5 µg/mL of linear
388 plasmid DNA was used for all reactions.

389

390 Fig. 6 shows the results of the digestion of DNA–H-NS complexes by NruI in the absence and
391 presence of PEG. NruI cleaves DNA into two fragments with around 3500 bp and 750 bp, as can be
392 seen in lane 3 of Fig. 6a. Again, panel (a) refers to control experiments in the absence of NruI
393 digestion, showing the mobility of DNA–H-NS complex formation in the absence (lanes 4 to 9) and
394 presence (lanes 10 to 15) of PEG. Panel (b) shows the results of the digestion of DNA in the
395 equivalent samples. It is interesting to note that, in this case, two bands with sizes corresponding to
396 the expected digestion fragments are observed for all tested samples, which indicate that H-NS does
397 not bind to these regions, or that it is easily displaced by the restriction enzyme. It is also observed
398 that PEG does not significantly improve the protection of DNA towards digestion.

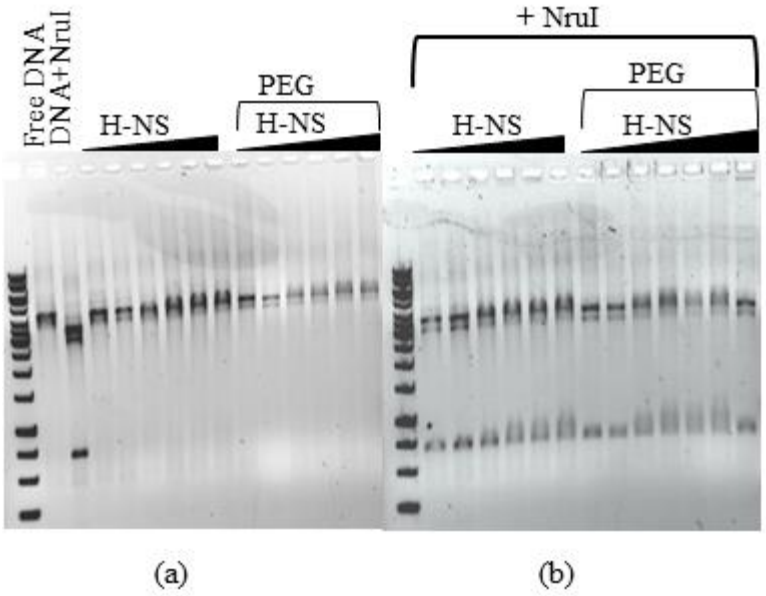


**Figure 6.** DNA foot printing assay. (a) Agarose gel electrophoresis of linear DNA with increasing H-NS concentrations 0.5, 1.0, 2.5, 5.0, 7.0, 10.0 µM (lanes 4 to 9) followed by the addition of 5 % crowding media PEG (lanes 10 to 15). Lanes 2 and 3 represent free DNA and DNA digested by NruI, respectively. (b) Agarose gel showing equivalent samples of DNA–H-NS and DNA–H-NS–PEG systems now treated with NruI enzyme. Lane 1 shows the ladder. A final concentration of 5 µg/mL of linear plasmid DNA was used for all reactions.

Results from the restriction digestion assays show two important aspects: H-NS prefers to bind near AT-rich and curved regions, and the presence of crowding decreases the concentration of H-NS needed for protecting these regions. On the other hand, PEG does not seen to affect the binding of H-NS to NruI binding site.

In addition, the production of green fluorescent protein (GFP) in the presence and absence of H-NS and PEG was followed by using an *in vitro* translation assay. The independent additions of H-NS and PEG to DNA led to a decrease in GFP expression, as described previously, but unfortunately,

the synergism of H-NS and PEG on gene regulation could not be concluded from the data (Table S1).

## DISCUSSION

**H-NS: DNA binding, protection and gene regulation:** As starting point to assess the synergistic effect of crowding on DNA-protein binding we began with evaluating the interactions of H-NS with DNA. From EMSA studies we see that at the lowest H-NS concentrations (0.5 μM) there is no change in the DNA band mobility and at 1 μM and above only a small retardation is observed (Fig. 2a). FCS experiments performed with H-NS concentrations up to 2 μM showed that DNA maintains a constant translational diffusion coefficient with varied H-NS concentration (Fig. 3a). This indicates that, under the used conditions, the presence of H-NS does not induce a significant DNA condensation. This was also confirmed by fluorescence lifetime measurements (FLIM) of DNA–H-NS complexes, where the presence of H-NS did not show significant change in the lifetime of fluorophore Alexa-488 tagged to DNA (data not shown), indicating that the environment of the probe did not change upon H-NS addition, opposite to what would be expected in case of strong DNA condensation. To attest DNA–H-NS complex formation for low H-NS simple digestion assays were conducted using DNase I, NruI and NdeI (Figs. 4 to 6). We observed that H-NS was shown to only partially protect DNA towards DNase I digestion, at concentration of 5 μM and above. NdeI digestion, on the other hand, was significantly reduced in the presence of just 0.5 μM and mostly inhibited for H-NS concentration of 2.5 μM and above. The same quantitative behavior was observed for the switching off of GFP synthesis, as seen in the in vitro transcription/translation assays (Table S1). Interestingly, the presence of H-NS did not affect NruI digestion of the DNA, for all studied concentrations. These results taken together suggest the following behavior: at very low H-NS concentration (1 μM and below), H-NS binds to the AT-rich tracks of DNA, protecting

these regions from NdeI digestion and blocking the transcription/translation of the GFP gene, but leaving most of the DNA chain naked and susceptible to digestion by DNase I. Under this regime, the conformation of DNA does not vary significantly, as observed from FCS and suggested by EMSA studies. This is in good agreement with recent reports showing that addition of H-NS does not change the hydrodynamic radius of DNA [38]. It has been shown that at the used $Mg^{2+}$ concentration, these ions mediate the formation of H-NS bridges between DNA segments and formation of hair-pin loop-like structures [21]. Such structures are not expected to affect the hydrodynamic radius of the DNA molecule to a big extent, also in good agreement with the FCS studies.

Further increase in H-NS concentration leads to the aggregation of multiple DNA chains, as indicated by FCS. It is unclear to us why such aggregation does not lead to a larger shift in the mobility of the bands in EMSA, but it may be due to the dissociation of complexes during the migration or while entering the gel. Atomic force micrographs in Fig. 7 confirm that the presence of 5 μM of H-NS leads to a moderate level of DNA condensation, where several DNA molecules are aggregated in a “flower-like” complex with apparent “naked” DNA strands forming loops and tails around the complex core. This is in excellent agreement with the only partial protection of H-NS towards DNA digestion by DNase I and NdeI.

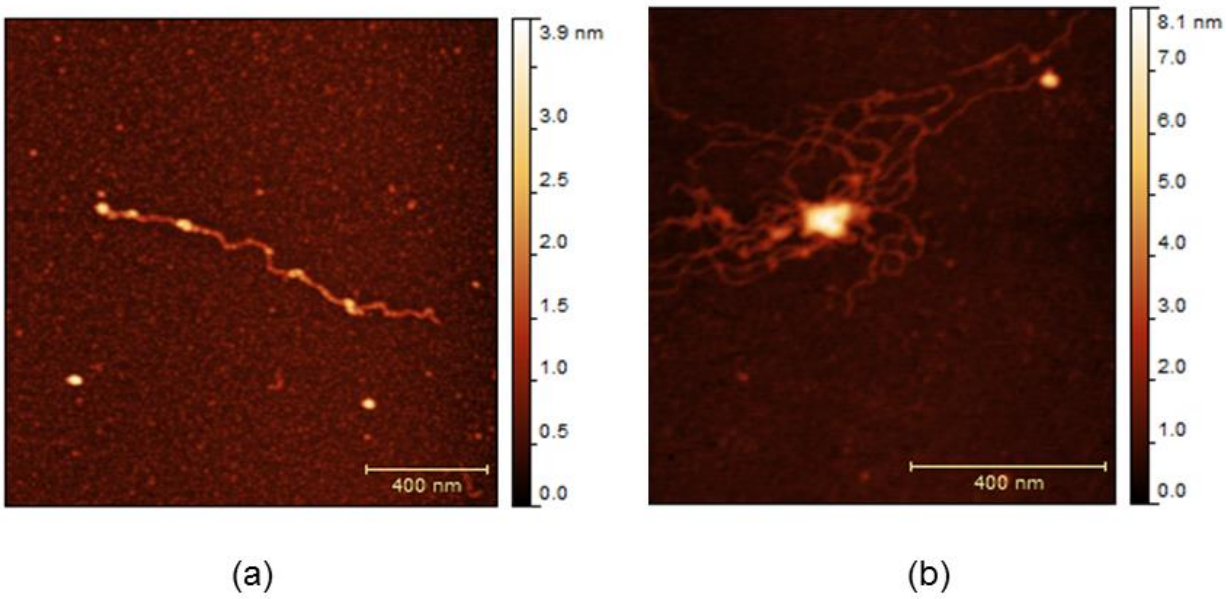


**Figure 7.** AFM images of DNA molecules in the absence (a) and presence (b) of 5 μM of H-NS.

**DNA condensation by crowding agent**

Ψ-condensation of DNA by PEG, due to excluded volume effects, is well-known. In order to assess the impact of excluded volume effects on DNA–proteins binding, control experiments on DNA condensation by PEG have also been performed.

In brief, and having in mind that the variations are almost within the margin of error, FCS results suggest an initial decrease in the dimensions of the DNA molecules, followed by an increase, probably due to DNA aggregation, with increasing concentrations of PEG. On the other hand, exclusion dye assays show that titration of plasmid DNA with increasing concentrations of PEG leads to a decrease in the dye fluorescence intensity, which for the chosen PEG concentration of 5 % amounts at about 30 % decrease in intensity (Fig. S1). This could indicate that the viscosity correction of the translational diffusion coefficient is too conservative. The condensation behavior of DNA could not be followed using EMSA since PEG, being a neutral polymer, stays in the wells during the electrophoretic run, as previously reported [42]. As such, and assuming that the system

474 is in equilibrium, the DNA band should show the same mobility in the presence and absence of PEG,
475 as it is observed.
476 DNase digestion studies show that DNA is completely digested. Since PEG does not directly bind
477 to DNA, it is not expected to provide as strong protection as DNA-binding agents, such as spermine
478 [41] and cationic dendrimers or surfactants [47].
479 When looking into the gene expression of the plasmid in the presence of PEG, it is found that there
480 is a significant decrease in the amount of produced GFP, as previously described [48].
481
482 **Synergistic role of PEG on DNA–H-NS interactions**
483 As mentioned above, these complex systems are challenging to study. Here we have unequivocally
484 shown, using FCS that the presence of PEG leads to more condensed DNA–H-NS complexes (Fig.
485 3b and Table 1).
486 The effect of crowding (excluded-volume effects) on the behavior of macromolecules can be divided
487 into two main classes: changes in the association rates of aggregation and binding to other
488 molecules; and changes in the conformational behavior of the macromolecule.
489 Taken together, our results suggest that both effects play a role in the observed synergism of
490 crowding in DNA – H-NS binding. The fact that DNA is protected towards digestion by DNase I
491 more efficiently than when only one of these agents is present (Fig. 4) indicates that there is some
492 degree of DNA condensation, which reduces the DNA availability to the enzyme. We recall that
493 PEG is not expected to bind directly to DNA or DNA–H-NS complexes. On the other hand, digestion
494 experiments conducted with NdeI and NruI suggest that PEG also affects the binding constant of H-
495 NS to DNA. NdeI and NruI possess different binding affinities to DNA sequences, with NdeI
496 cleaving AT-rich sequences, also the preferential binding site to H-NS [49]. As shown in Figs. 5 and

6, PEG hinders DNA digestion by NdeI at lower H-NS concentrations, while it does not seem to affect the H-NS binding to GC-rich tracks of DNA and hence digestion by NruI.

It is not clear to us why DNase activity is blocked, while digestion by NruI proceeds but could be related to the differences in composition of the reaction buffer of the restriction enzymes, which contain BSA, for example (see NEB protocols for NdeI and NruI). Translation experiments of GFP expression showed a decrease in GFP expression for DNA and DNA–H-NS complexes in the presence of crowding molecules, although the synergism of H-NS and PEG on the biological activity of DNA could not be concluded from these experiments due to relatively large variations between independent sample sets and concomitantly large error bars.

It has been suggested, based on theoretical arguments, that DNA condensation in the presence of DNA-binding proteins and crowding agents is promoted by the larger diameter and partial neutralization of the DNA filaments when compared to DNA alone. We further suggest that synergistic effects are stronger when DNA–H-NS complexes have a curved or looped structure ("flower-like" complexes). Recent studies on the diffusion of single DNA molecules in a crowding environment have shown that circular DNA (relaxed plasmid) is more prone to condensation than linear molecules [50].

**Considerations on the role of $Mg^{2+}$ on DNA condensation**

The presence of divalent ions affects the binding mode of H-NS to DNA. It has been shown that the presence of magnesium ions promotes the formation of bridges between DNA segments, mediated by H-NS dimers, while in the absence of divalent ions H-NS polymerases along the DNA chain, increasing its stiffness [21]. To better understand the impact of $Mg^{2+}$ on the synergism of H-NS and PEG on DNA condensation we have performed all described experiments with a binding buffer

without $Mg^{2+}$. We summarize here our observations. FCS experiments performed with the same H-NS and PEG concentration ranges presented in this work but performed in the absence of $Mg^{2+}$, showed no improved DNA condensation in the presence of PEG (not shown). Accordingly, EMSA showed no mobility shift in the DNA band in the presence of either H-NS and/or PEG.

DNase digestion assays showed partial protection of the DNA in the presence of H-NS which is consistent with the formation of protein filaments along the DNA strands. Furthermore, the presence of PEG led to a stronger protection (Fig. S4), which is in agreement with the proposed mechanism that the crowding leads to an increased association of the H-NS along the DNA. Unfortunately, it was not possible to perform NdeI and NruI digestion assays in the absence of $Mg^{2+}$ since these enzymes require $Mg^{2+}$ to function. The *in vitro* transcription/translation experiments were not attempted since the reaction buffer also contains divalent ions.

We suggest that the formation of DNA loops, induced by the H-NS in the presence of $Mg^{2+}$, aids in DNA condensation in the presence of PEG. It has been suggested that H-NS filaments (in the absence of $Mg^{2+}$) can also promote DNA bridging and concomitant loop formation; however, such structures will increase the stiffness of DNA, which could explain why we have not observed synergism in DNA condensation in the absence of $Mg^{2+}$. We have additionally performed dye exclusion experiments to assess the effect of 10 mM $MgCl_2$ on DNA condensation by PEG and found that, as expected, the $Mg^{2+}$ enhances the DNA ψ-condensation induced by PEG (not shown), although there was no increased protection of the DNA towards DNase digestion (lane 9 Fig. 4).

In conclusion, synergism in DNA condensation induced by binding and crowding agents is more predominant in the presence of 10 mM of the divalent ion, $Mg^{2+}$, probably due to the bridging binding mode of H-NS to the DNA, which induces the formation of DNA loops without increasing

significantly its stiffness. The presence of the $Mg^{2+}$ may, in addition, reduce the electrostatic repulsions in the DNA chains leading to a more efficient ψ-condensation.

Throughout this work we have considered the PEG molecules solely as crowding agents, that is, we have assumed that their action in solely due to excluded volume effects. It is known that PEG decreases the electric constant of the medium; however such variation was shown to be very mild for PEG concentrations below 10% and using relatively short PEG molecules [51]. It is undeniable that the crowding environment in a cell, mostly composed of proteins with different sizes, shapes and charge, is far more complicated than that given by roughly monodisperse neutral polymer molecules. Therefore, it is not surprising that differences arise when using solutions of inert polymers and cell extracts [52, 53]. Study of the synergistic effect of DNA-binding agents and a crowded environment in DNA condensation in the presence of cell extracts, will be a natural evolution of these investigations.

## CONCLUSIONS

Most biochemical reactions studied *in vitro* are performed without a crowding milieu, despite the fact that crowding can have a tremendous impact on the conformational states and association rates of bio macromolecules. Here we have investigated the synergistic effect of DNA-binding proteins and crowding agents on DNA condensation. Our results demonstrate that the crowding conditions of bacterial cells can contribute to the condensation and function of the nucleoid by both affecting the conformation of the genome and enhancing the binding of H-NS to certain sites in the genome. When added at low concentrations, H-NS does not change the conformation of DNA but partially protects its AT-rich sequences, towards digestion by a restriction enzyme and blocks its transcription activity. Increasing H-NS concentration leads to the aggregation of DNA molecules into flower-like

structure possessing partially naked DNA strands, and thus susceptible to digestion by DNase I. The presence of a crowded environment, mimicked by the addition of PEG molecules, leads to an increase in the protection against digestion of the AT-rich regions (though not of GC regions) of DNA, the switching off of GFP production, and a shift, to lower H-NS concentrations, of the DNA condensation and aggregation behavior.

## AUTHOR CONTRIBUTIONS

SRK and RSD conceived and designed the research. RL designed the DNA template and was involved in guidance of SRK in foot printing experiments. SRK, PL performed experiments. SRK, PL, and RSD analyzed the data. SRK and RSD wrote the manuscript.

## ACKNOWLEDGEMENTS

We acknowledge Prof. William Wiley Navarre for kindly providing us $P^{SSA2}$ plasmid for purification of H-NS. We thank Dr. Astrid Bjørkøy and Dr. Gjertrud Maurstad for their assistance with FCS and AFM measurements, respectively. This work was supported by the Norwegian University of Science and Technology.

## REFERENCES

[1] J.O. Thomas, R.D. Kornberg, An octamer of histones in chromatin and free in solution, Proceedings of the National Academy of Sciences of the United States of America 72(7) (1975) 2626-2630.
[2] C. Robinow, E. Kellenberger, The bacterial nucleoid revisited, Microbiological Reviews 58(2) (1994) 211-232.
[3] J.K. Fisher, A. Bourniquel, G. Witz, B. Weiner, M. Prentiss, N. Kleckner, Four-Dimensional Imaging of E. coli Nucleoid Organization and Dynamics in Living Cells, Cell 153(4) (2013) 882-895.
[4] L. Postow, C.D. Hardy, J. Arsuaga, N.R. Cozzarelli, Topological domain structure of the Escherichia coli chromosome, Genes & Development 18(14) (2004) 1766-1779.

[5] O. Espeli, R. Mercier, F. Boccard, DNA dynamics vary according to macrodomain topography in the E. coli chromosome, Molecular Microbiology 68(6) (2008) 1418-1427.
[6] D.C. Grainger, D. Hurd, M.D. Goldberg, S.J.W. Busby, Association of nucleoid proteins with coding and non-coding segments of the Escherichia coli genome, Nucleic Acids Research 34(16) (2006) 4642-4652.
[7] M.Y. Tolstorukov, K. Virnik, V.B. Zhurkin, S. Adhya, Organization of DNA in a bacterial nucleoid, BMC Microbiology 16(1) (2016) 22.
[8] C.W. Tabor, H. Tabor, Polyamines in microorganisms, Microbiological Reviews 49(1) (1985) 81-99.
[9] a. C W Tabor, H. Tabor, Polyamines, Annual Review of Biochemistry 53(1) (1984) 749-790.
[10] A. Nakabachi, H. Ishikawa, Polyamine Composition and Expression of Genes Related to Polyamine Biosynthesis in an Aphid Endosymbiont,Buchnera, Applied and Environmental Microbiology 66(8) (2000) 3305-3309.
[11] M. Joyeux, In vivo compaction dynamics of bacterial DNA: A fingerprint of DNA/RNA demixing?, Current Opinion in Colloid & Interface Science 26 (2016) 17-27.
[12] D.E. Pettijohn, Structure and properties of the bacterial nucleoid, Cell 30 (1982).
[13] M.S. Luijsterburg, M.C. Noom, G.J.L. Wuite, R.T. Dame, The architectural role of nucleoid-associated proteins in the organization of bacterial chromatin: A molecular perspective, Journal of Structural Biology 156(2) (2006) 262-272.
[14] F. Hommais, E. Krin, C. Laurent-Winter, O. Soutourina, A. Malpertuy, J.-P. Le Caer, A. Danchin, P. Bertin, Large-scale monitoring of pleiotropic regulation of gene expression by the prokaryotic nucleoid-associated protein, H-NS, Molecular Microbiology 40(1) (2001) 20-36.
[15] T.H. Kawula, P.E. Orndorff, Rapid site-specific DNA inversion in Escherichia coli mutants lacking the histonelike protein H-NS, Journal of Bacteriology 173(13) (1991) 4116-4123.
[16] H. Yamada, T. Yoshida, K.-i. Tanaka, C. Sasakawa, T. Mizuno, Molecular analysis of the Escherichia coli has gene encoding a DNA-binding protein, which preferentially recognizes curved DNA sequences, Molecular and General Genetics MGG 230(1) 332-336.
[17] R. Cukier-Kahn, M. Jacquet, F. Gros, Two Heat-Resistant, Low Molecular Weight Proteins from Escherichia coli That Stimulate DNA-Directed RNA Synthesis, Proceedings of the National Academy of Sciences of the United States of America 69(12) (1972) 3643-3647.
[18] M. Falconl, M.T. Gualtierl, A. La Teana, M.A. Losso, C.L. Pon, Proteins from the prokaryotic nucleoid: primary and quaternary structure of the 15-kD Escherichia coli DNA binding protein H-NS, Molecular Microbiology 2(3) (1988) 323-329.
[19] S. Ceschini, G. Lupidi, M. Coletta, C.L. Pon, E. Fioretti, M. Angeletti, Multimeric Self-assembly Equilibria Involving the Histone-like Protein H-NS: A THERMODYNAMIC STUDY, Journal of Biological Chemistry 275(2) (2000) 729-734.
[20] R.T. Dame, C. Wyman, N. Goosen, H-NS mediated compaction of DNA visualised by atomic force microscopy, Nucleic Acids Research 28(18) (2000) 3504-3510.
[21] Y. Liu, H. Chen, L.J. Kenney, J. Yan, A divalent switch drives H-NS/DNA-binding conformations between stiffening and bridging modes, Genes & Development 24(4) (2010) 339-344.
[22] R.T. Dame, M.C. Noom, G.J.L. Wuite, Bacterial chromatin organization by H-NS protein unravelled using dual DNA manipulation, Nature 444(7117) (2006) 387-390.
[23] M. Joyeux, J. Vreede, A Model of H-NS Mediated Compaction of Bacterial DNA, Biophysical Journal 104(7) (2013) 1615-1622.

[24] V. Bloch, Y. Yang, E. Margeat, A. Chavanieu, M.T. Auge, B. Robert, S. Arold, S. Rimsky, M. Kochoyan, The H-NS dimerization domain defines a new fold contributing to DNA recognition, Nat Struct Mol Biol 10(3) (2003) 212-218.
[25] J.M. Lucht, P. Dersch, B. Kempf, E. Bremer, Interactions of the nucleoid-associated DNA-binding protein H-NS with the regulatory region of the osmotically controlled proU operon of Escherichia coli, Journal of Biological Chemistry 269(9) (1994) 6578.
[26] S.B. Zimmerman, L.D. Murphy, Macromolecular crowding and the mandatory condensation of DNA in bacteria, FEBS Letters 390(3) (1996) 245-248.
[27] S.B. Zimmerman, S.O. Trach, Estimation of macromolecule concentrations and excluded volume effects for the cytoplasm of Escherichia coli, Journal of Molecular Biology 222(3) (1991) 599-620.
[28] H.-X. Zhou, G. Rivas, A.P. Minton, Macromolecular Crowding and Confinement: Biochemical, Biophysical, and Potential Physiological Consequences, Annual Review of Biophysics 37(1) (2008) 375-397.
[29] a. S B Zimmerman, A.P. Minton, Macromolecular Crowding: Biochemical, Biophysical, and Physiological Consequences, Annual Review of Biophysics and Biomolecular Structure 22(1) (1993) 27-65.
[30] R.J. Ellis, Macromolecular crowding: obvious but underappreciated, Trends in Biochemical Sciences 26(10) (2001) 597-604.
[31] A.P. Minton, The Influence of Macromolecular Crowding and Macromolecular Confinement on Biochemical Reactions in Physiological Media, Journal of Biological Chemistry 276(14) (2001) 10577-10580.
[32] L.S. Lerman, A Transition to a Compact Form of DNA in Polymer Solutions, Proceedings of the National Academy of Sciences of the United States of America 68(8) (1971) 1886-1890.
[33] A.Y. Grosberg, I.Y. Erukhimovitch, E.I. Shakhnovitch, On the theory of Ψ-condensation, Biopolymers 21(12) (1982) 2413-2432.
[34] J.É.B. Ramos, J.R. Neto, R. de Vries, Polymer induced condensation of DNA supercoils, The Journal of Chemical Physics 129(18) (2008) 185102.
[35] V.V. Vasilevskaya, A.R. Khokhlov, Y. Matsuzawa, K. Yoshikawa, Collapse of single DNA molecule in poly(ethylene glycol) solutions, The Journal of Chemical Physics 102(16) (1995) 6595-6602.
[36] L.D. Murphy, S.B. Zimmerman, Macromolecular crowding effects on the interaction of DNA with Escherichia coli DNA-binding proteins: A model for bacterial nucleoid stabilization, Biochimica et Biophysica Acta (BBA) - Gene Structure and Expression 1219(2) (1994) 277-284.
[37] e. Bessa ramos, k. Wintraecken, a. Geerling, and r. De vries., Synergy of DNA-bending nucleoid proteins and macromolecular crowding in condensing DNA, Biophysical Reviews and Letters Volume 02,(Issue 03n04,) (October 2007).
[38] A.S. Wegner, K. Wintraecken, R. Spurio, C.L. Woldringh, R. de Vries, T. Odijk, Compaction of isolated Escherichia coli nucleoids: Polymer and H-NS protein synergetics, J Struct Biol 194(1) (2016) 129-37.
[39] S.S. Ali, E. Beckett, S.J. Bae, W.W. Navarre, The 5.5 Protein of Phage T7 Inhibits H-NS through Interactions with the Central Oligomerization Domain, Journal of Bacteriology 193(18) (2011) 4881-4892.
[40] G. Chirico, J. Langowski, Kinetics of DNA supercoiling studied by Brownian dynamics simulation, Biopolymers 34(3) (1994) 415-433.

[41] S.K. Ramisetty, R.S. Dias, Synergistic role of DNA-binding protein and macromolecular crowding on DNA condensation. An experimental and theoretical approach, Journal of Molecular Liquids 210, Part A (2015) 64-73.
[42] S. Hou, P. Trochimczyk, L. Sun, A. Wisniewska, T. Kalwarczyk, X. Zhang, B. Wielgus-Kutrowska, A. Bzowska, R. Holyst, How can macromolecular crowding inhibit biological reactions? The enhanced formation of DNA nanoparticles, Scientific Reports 6 (2016) 22033.
[43] R.S. Dias, J. Innerlohinger, O. Glatter, M.G. Miguel, B. Lindman, Coil−Globule Transition of DNA Molecules Induced by Cationic Surfactants: A Dynamic Light Scattering Study, The Journal of Physical Chemistry B 109(20) (2005) 10458-10463.
[44] S.S. Singh, D.C. Grainger, H-NS Can Facilitate Specific DNA-binding by RNA Polymerase in AT-rich Gene Regulatory Regions, PLoS Genet 9(6) (2013) e1003589.
[45] B.R.G. Gordon, Y. Li, A. Cote, M.T. Weirauch, P. Ding, T.R. Hughes, W.W. Navarre, B. Xia, J. Liu, Structural basis for recognition of AT-rich DNA by unrelated xenogeneic silencing proteins, Proceedings of the National Academy of Sciences 108(26) (2011) 10690-10695.
[46] E. Bouffartigues, M. Buckle, C. Badaut, A. Travers, S. Rimsky, H-NS cooperative binding to high-affinity sites in a regulatory element results in transcriptional silencing, Nat Struct Mol Biol 14(5) (2007) 441-448.
[47] M.-L. Ainalem, A. Bartles, J. Muck, R.S. Dias, A.M. Carnerup, D. Zink, T. Nylander, DNA Compaction Induced by a Cationic Polymer or Surfactant Impact Gene Expression and DNA Degradation, PLoS ONE 9(3) (2014) e92692.
[48] X. Ge, D. Luo, J. Xu, Cell-Free Protein Expression under Macromolecular Crowding Conditions, PLoS ONE 6(12) (2011) e28707.
[49] B. Lang, N. Blot, E. Bouffartigues, M. Buckle, M. Geertz, C.O. Gualerzi, R. Mavathur, G. Muskhelishvili, C.L. Pon, S. Rimsky, S. Stella, M.M. Babu, A. Travers, High-affinity DNA binding sites for H-NS provide a molecular basis for selective silencing within proteobacterial genomes, Nucleic Acids Research 35(18) (2007) 6330-6337.
[50] S.M. Gorczyca, C.D. Chapman, R.M. Robertson-Anderson, Universal scaling of crowding-induced DNA mobility is coupled with topology-dependent molecular compaction and elongation, Soft Matter 11(39) (2015) 7762-7768.
[51] K. Arnold, A. Herrmann, L. Pratsch, K. Gawrisch, The dielectric properties of aqueous solutions of poly(ethylene glycol) and their influence on membrane structure, Biochim Biophys Acta 815(3) (1985) 515-518.
[52] A.H. Elcock, Models of macromolecular crowding effects and the need for quantitative comparisons with experiment, Current Opinion in Structural Biology 20(2) (2010) 196-206.
[53] J. Groen, D. Foschepoth, E. te Brinke, A.J. Boersma, H. Imamura, G. Rivas, H.A. Heus, W.T.S. Huck, Associative Interactions in Crowded Solutions of Biopolymers Counteract Depletion Effects, Journal of the American Chemical Society 137(40) (2015) 13041-13048.